

# Correlated two-pion exchange and large- $N_c$ behavior of nuclear forces

Murat M. Kaskulov\* and Heinz Clement†

*Physikalisches Institut, Universität Tübingen, D-72076 Tübingen, Germany*

(Dated: October 30, 2018)

## Abstract

The effect of correlated scalar-isoscalar two-pion exchange (CrTPE) modes is considered in connection with central and spin-orbit parts of the  $NN$  force. The two-pion correlation function is coupled directly to the scalar form factor of the nucleon which we calculate in the large- $N_c$  limit where the nucleon can be described as a soliton of an effective chiral theory. The results for the central  $NN$  force show a strong repulsive core at short internucleon distances supplemented by a moderate attraction beyond 1 fm. The long-range tail of the central  $NN$  potential is driven by the pion-nucleon sigma term and consistent with the effective  $\sigma$  meson exchange. The spin-orbit part of the  $NN$  potential is repulsive. The large- $N_c$  scaling behavior of the scalar-isoscalar  $NN$  interaction is addressed. We show that the spin-orbit part is  $\mathcal{O}(1/N_c^2)$  in strength relative to the central force resulting in the ratio  $\simeq 1/9$  suggested by the  $1/N_c$  expansion for  $N_c = 3$ . The latter is in agreement with our numerical analysis and with the Kaplan-Manohar large- $N_c$  power counting. Unitarization of the  $\pi\pi$  scattering amplitude plays here an important role and improves the tree level results. Analytical representations of the CrTPE  $NN$  potential in terms of elementary functions are derived and their chiral content is discussed.

---

\*Electronic address: kaskulov@pit.physik.uni-tuebingen.de

†Electronic address: clement@pit.physik.uni-tuebingen.de

## I. INTRODUCTION

Understanding the intermediate and short range parts of the nucleon-nucleon ( $NN$ ) interaction is still an interesting problem and much effort is being put into this topic both from theoretical and from experimental sides. The long-range part of the  $NN$  interaction is well described and represented by means of the one-pion-exchange (OPE) potential. For higher momentum transfer or small internucleon distances the  $NN$  dynamics becomes complex and one has to rely on phenomenological models. In this region the  $\sigma$  meson [1], for which the empirical evidence remains controversial, effectively represents scalar-isoscalar multi-pion correlations and generates an intermediate range attraction in microscopic QCD motivated approaches [2, 3] and one-boson-exchange (OBE) models [4, 5]. The latter are most popular and phenomenologically successful in describing the nuclear force.

With the recent progress of chiral perturbation theory ( $\chi$ PT) in meson-meson and meson-baryon sectors the idea to extend it to the description of the  $NN$  interaction appears to be quite natural. The chiral  $SU_L(N_f) \times SU_R(N_f)$  symmetry provides a consistent framework for the construction of the  $NN$  force [6, 7, 8]. In  $\chi$ PT the  $NN$  potential has already been calculated in  $N^3LO$  [9, 10] and much work has been done in applying these ideas to nuclei, too. Supported by empirical information [11], the  $\chi$ PT calculations are important and transparent for the peripheral  $NN$  partial waves, which are well understood in terms of OPE and two-pion-exchange (TPE) processes [8, 11, 12]. The long-range behavior of the TPE force and the effect of correlated  $\sigma$ -like scalar-isoscalar  $\pi\pi$  modes are related problems. The success and dynamical content of OBE models suggest that meson-meson correlations are important [13, 14]. This fact is motivated by dispersion theory, where the main effects of higher-order interactions can be accounted for by the inclusion of experimentally known meson resonances, which bring singularities of the amplitude close to the physical region. In the dispersion-theoretical framework, the  $\sigma$  can be explained by correlated two-pion exchange with a broad spectral distribution around  $\simeq 4M_\pi$  which ultimately leads to the isoscalar central attraction between two nucleons.

In baryon  $\chi$ PT the  $\pi\pi$  correlations are taken into account at tree level and the relation to the genuine  $\sigma$  exchange is lost. For example, in heavy baryon  $\chi$ PT the exchange of two uncorrelated pions, formulated using chiral symmetry constraints and including  $\Delta$  isobars, explains the tail of the scalar-isoscalar  $NN$  potential without any need for a true scalar meson [15]. Additional

consideration of tree level  $\pi\pi$  correlations leads to the surprising result, that these terms are very small and - even more - lead to a weak repulsion [15]. Note, that in the effective theory without explicit  $\Delta$  degrees of freedom the chiral invariant  $NN$  interaction terms are accompanied in subleading order by low-energy constants (LEC)  $c_1, c_3$  and  $c_4$  [16]. In particular, the isoscalar central potential is dominated by  $c_1$  and  $c_3$  [8, 11] proportional to the pion-nucleon sigma term and nucleon axial-polarizability, respectively. The LEC  $c_3$  can be approximately saturated by the  $\Delta$  resonance. But the dimension-two operators  $c_i$  include also information about  $t$ -channel meson exchange suggesting a strong influence of  $t$ -channel singularities. The latter was studied in Refs. [17, 18] (see also Ref. [16]) where it was shown that the exchange of a scalar meson with mass and coupling constant similar to  $\sigma$  allows to explain  $c_1$  and, interestingly, also part of  $c_3$ . Finally,  $c_4$  mentioned above is dominated by isovector  $\pi\pi$  correlations from  $\rho$  meson exchange [17]. Since we concentrate in this paper on  $s$ -wave CrTPE, i.e.  $\sigma$ - meson channel, in the following we will discuss matters predominantly connected with  $c_1$ .

As well known the tree level contact interaction does not account for the entire  $\pi\pi$  dynamics, and possibly one has to go beyond the tree level approximation to restore the relation to the  $\sigma$  meson. Recently, non-perturbative methods describing  $\pi\pi$  scattering were developed [19, 20, 21, 22, 23, 24]. One of them was proposed in Ref. [25], where based on the Bethe-Salpeter description of the  $\pi\pi$  scattering process the re-summation of the infinite series of pion loops was suggested. This method which only uses the lowest order chiral Lagrangian as input and implements an exact unitarity, leads to a dynamical pole in the  $\pi\pi$  amplitude with a position around  $M - i\Gamma/2 \simeq 450 - i221$  MeV. Naturally, it is identified with the  $\sigma$  meson. Considering the role played by the unitary  $\pi\pi$  correlations (or dynamical  $\sigma$  state) in the  $NN$  interaction problem, it was found [26] that the resulting scalar-isoscalar central  $NN$  potential shows a strong repulsion at internucleon distances less then  $\sim 1$  fm, and a moderate attraction at  $r > 1$  fm. This feature of unitary  $\pi\pi$  scalar-isoscalar correlations differs from the conventional Yukawa-like  $\sigma$  exchange,  $V_\sigma(r) \sim -\exp(-m_\sigma r)/r$ , which always results in an attraction. Interestingly, in phenomenological  $NN$  interaction models like Paris [27], Argonne V18 [28], Nijmegen [29] and CD-Bonn [30] the isospin independent scalar components are rather similar for  $NN$  separations beyond 0.5 fm [31]. But the radial dependencies differ considerably at short distances, ranging from attractive for Nijmegen and CD-Bonn (by construction) to repulsive for the more phenomenological V18 and Paris potentials. It also was argued that the appearance of a strong repulsion in the scalar-isoscalar channel cannot be

interpreted in terms of meson exchange [31], a remarkable feature which only was known from the Skyrme model [32] and now from Ref. [26]. It is instructive, that in the Skyrme model the use of the simplest product ansatz results in a repulsive central force [33], and the missing intermediate range attraction can be produced only if one goes beyond the product approximation [34] or additionally considers the correlated two-pion exchange (CrTPE) in the scalar-isoscalar channel [35].

In this work the role played by the CrTPE in the  $NN$  interaction is reconsidered for the construction of the scalar-isoscalar central and spin-orbit  $NN$  potentials. Considering the tree level and unitary two-pion correlations in the  $NN$  interaction problem, we couple the  $\pi\pi$  correlation function to the scalar form factor of the nucleon in a model-independent way. The latter is calculated in the limit of a large number of colors (large- $N_c$  limit) using the Chiral Quark-Soliton Model ( $\chi$ QSM) [36, 37] where the nucleon can be described as a soliton of an effective chiral theory. This way our results support the structure of the scalar-isoscalar central  $NN$  force observed in the unitarized  $\chi$ PT [26] and in the Skyrme model [34]. We find a strong repulsion at short distances and a moderate attraction at  $r > 1$  fm - even with the tree level  $\pi\pi$  interaction. The tail of the central CrTPE potential is driven by the the pion-nucleon ( $\pi N$ ) sigma term and is consistent with the effective  $\sigma$  exchange in OBE models. By this, the effective  $\sigma NN$  coupling constant can be related to the  $\pi N$  sigma term. We also show that the above feature of the central  $NN$  force is general. It mainly relies on the particular functional form of the scalar form factor of the nucleon and is not the effect of unitarization. Another point of interest in this work is the generation of the scalar-isoscalar spin-orbit ( $LS$ ) force. Our results for this part of the  $NN$  potential show a repulsion - a feature which differs from phenomenological  $\sigma$  exchange resulting in an attractive  $LS$  interaction.

The large- $N_c$  behavior of CrTPE forces is considered and consistency with large- $N_c$  QCD analyses and the large- $N_c$  behavior of scalar-isoscalar components of phenomenological  $NN$  interaction models is shown. Both, the central and spin-orbit parts satisfy large- $N_c$  QCD counting rules. We find that the relative strength of spin-orbit and central interactions scales according to  $\simeq 1/9$  in remarkable agreement with the Kaplan-Manohar large- $N_c$  spin-flavor power counting [38]. Additionally, analytical representations of central and  $LS$  potentials in terms of elementary functions are derived and their chiral content is discussed. We show that the chiral symmetry breaking part of the interaction is small and that terms non-vanishing in the chiral limit are dominant and fully drive all essential features of the CrTPE force in the scalar-isoscalar channel.

The paper is organized as follows. In the next two sections we discuss the construction of the CrTPE scalar-isoscalar  $NN$  force. We emphasize the importance of the scalar form factor of the nucleon and give its phenomenological description in Sec. V. The large- $N_c$  scaling and consistency are addressed in Sec. IV. Finally, the analytical results and discussions are presented in Sec. VI.

## II. TWO-PION CORRELATION FUNCTION

We start our considerations of the scalar-isoscalar CrTPE  $NN$  interaction from the standard definition of the tree level  $\pi\pi$  correlation function and its large- $N_c$  behavior. To lowest order in the derivative expansion the mesonic Lagrangian  $\mathcal{L}_\pi^{(2)}$  is given by the  $SU(3)$  nonlinear  $\sigma$  model

$$\mathcal{L}_\pi^{(2)} = \frac{f_\pi^2}{4} \text{Tr} \left[ \partial^\mu U^\dagger \partial_\mu U \right] + \mathcal{B} \frac{f_\pi^2}{2} \text{Tr} \left[ \mathcal{M}(U + U^\dagger) \right] \quad (1)$$

and contains the most general low-energy interactions of the pseudo-scalar meson octet. In Eq. (1) the leading symmetry-breaking term is linear in the quark masses  $\mathcal{M}$  and is characterized by  $\mathcal{B} = -\langle q\bar{q} \rangle / f_\pi^2$ . The pion-decay constant  $f_\pi = 93$  MeV and the scalar condensate  $\langle q\bar{q} \rangle$  are the relevant parameters. In the  $SU(2)$  limit the non-linear field  $U$  entering Eq. (1) is given by the standard matrix form:

$$U(x) = \exp \left( i\Phi(x)/f_\pi \right), \quad \Phi \equiv \boldsymbol{\tau} \boldsymbol{\pi} \quad (2)$$

where  $\boldsymbol{\tau}$  are the  $SU(2)$  Pauli matrices and  $\boldsymbol{\pi}$  is the isovector pion field. For the  $\pi_a \pi_b \rightarrow \pi_c \pi_d$  scattering process, defined by the Cartesian isospin indices  $a, \dots$ , the use of the standard  $\chi$ PT procedure in expanding the  $\mathcal{L}_\pi^{(2)}$  to order  $\mathcal{O}(\boldsymbol{\pi}^4)$  results in the tree level contact interaction

$$-iV_{\pi\pi}^{ab \rightarrow cd} = \delta_{ab}\delta_{cd}A(s) + \delta_{ac}\delta_{bd}A(t) + \delta_{ad}\delta_{bc}A(u), \quad (3)$$

where

$$A(s) = \frac{i}{f_\pi^2} \left( s - M_\pi^2 - \frac{1}{3} \sum_{i=a,b,c,d} \Lambda_i \right) + \mathcal{O}(q^4), \quad (4)$$

and  $\Lambda_i = k_i^2 - M_\pi^2$  are the off-shell part of the invariant  $\pi\pi$  amplitude. The Mandelstam variables are related by  $s + t + u = k_a^2 + k_b^2 + k_c^2 + k_d^2$ . At this order of the pion field expansion the isoscalar  $S$ -wave  $\pi\pi$  partial amplitude ( $L = 0$ ) is obtained from the standard decomposition

$$V_{\pi\pi}^{L,I=0} = \frac{1}{2} \frac{1}{(\sqrt{2})^\alpha} \int_{-1}^1 d\cos\theta \ P_L(\cos\theta) \ V_{\pi\pi}^{I=0}(\theta) \quad (5)$$

where  $P_L(\cos\theta)$  are the Legendre polynomials and  $(\sqrt{2})^\alpha$  accounts for the statistical factor occurring in states with identical particles:  $\alpha = 2$  for  $\pi\pi \rightarrow \pi\pi$ . The tree level scalar-isoscalar  $\pi\pi$

scattering amplitude is

$$V_{\pi\pi}^{L=I=0} = -\frac{1}{f_\pi^2} \left( s - \frac{M_\pi^2}{2} - \frac{1}{3} \sum_i \Lambda_i \right). \quad (6)$$

In the limit of a large number of colors  $N_c$  of QCD, the scaling behavior of Eq. (6) can be obtained from large- $N_c$   $\chi$ PT [39]. The conventional large- $N_c$  counting rules require that the pion mass is  $M_\pi \sim \mathcal{O}(1)$  and the decay constant is  $f_\pi \sim \mathcal{O}(\sqrt{N_c})$ . As a result the  $\pi\pi$  amplitude scales according to

$$V_{\pi\pi} \sim \mathcal{O}(1/N_c) \quad (7)$$

and large- $N_c$  QCD becomes a theory of weakly interacting pions. Note that the unitarization of the  $\pi\pi$  correlation function (scattering amplitude)  $V_{\pi\pi}^{L=I=0}$ , Eq. (6), is a lengthy procedure. Here, we only mention some recent analyses which employ dispersion relations [21], Padé approximants [22], solution of Roy [23] and Bethe-Salpeter [24, 25] equations. Unitary  $\pi\pi$  scattering amplitudes as provided by most of these methods contain a dynamical pole [20] which is identified with the  $\sigma$  meson.

### III. TWO-PION EXCHANGE KERNEL AND SCALAR FORM FACTOR

With Eq. (6) we come to the definition of the CrTPE potential in the scalar-isoscalar channel describing the on-shell  $NN$  scattering process,  $N(p_1, s_1)N(p_2, s_2) \rightarrow N(p_3, s_3)N(p_4, s_4)$ , where  $p_i$  and  $s_i$  are the four momenta and spins of interacting nucleons, respectively. As well known, in the generic case of TPE the chiral symmetry constraints work best and allow to relate the TPE process containing two intermediate pions, with Cartesian isospin indices  $a$  and  $b$  to the off-mass shell  $\pi N$  scattering amplitude in a model-independent way [8, 10, 40]. The latter is defined by the Green function [41]:

$$\begin{aligned} \mathcal{G}_{\pi N} &= i \int \int d^4x \, d^4y \, \langle p', s' | \hat{T} P^a(x) P^b(y) | p, s \rangle e^{i(k'x - ky)} \\ &= \frac{G_\pi}{k^2 - M_\pi^2} \frac{G_\pi}{k'^2 - M_\pi^2} T_{\pi N}^{ab}(p', k', p, k) \end{aligned} \quad (8)$$

Here  $G_\pi$  accounts for the coupling of the pion field to the pseudoscalar quark densities  $\langle 0 | P^a(0) | \pi^b \rangle = \delta_{ab} G_\pi$ ,  $P^a(x) = i\bar{\psi}(x)\gamma_5\tau^a\psi(x)$  and  $p', p$  ( $k', k$ ) are the momenta of outgoing and incoming nucleons (pions). For the  $\pi N$  scattering amplitude  $T_{\pi N}^{ab}$  the standard decomposition involves four Lorentz invariant functions  $D^\pm, B^\pm$ :

$$T_{\pi N}^{ab} = \delta_{ab} F_{\pi N}^+ + \frac{1}{2} [\tau_a, \tau_b] F_{\pi N}^-, \quad (9)$$

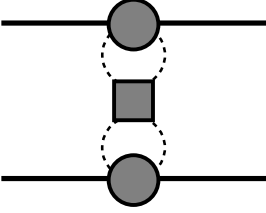


FIG. 1: The coupling of the scalar-isoscalar  $\pi\pi$  correlation function  $V_{\pi\pi}^{L=I=0}$  (filled box) to the isospin symmetric part  $F_{\pi N}^+$  (filled disk) of the  $\pi N$  scattering amplitude.

$$F_{\pi N}^\pm = \bar{u}(p'_N, s') \left[ D^\pm + i\sigma^{\mu\nu} k'_\mu k'_\nu B^\pm \right] u(p_N, s). \quad (10)$$

We are interested in the chiral content of the TPE potential in the scalar-isoscalar channel where the introduction of the tree level contact  $\pi\pi$  interaction results in a  $NN$  scattering amplitude with two connected pion loops

$$\begin{aligned} -i\mathcal{V}_{NN} = & i \left( \frac{3}{2} \right) \int \int \frac{d^4 k}{(2\pi)^4} \frac{d^4 \tilde{k}}{(2\pi)^4} \left( V_{\pi\pi}^{L=I=0} \right) \\ & \times \left[ \frac{[F_{\pi N}^+]^{(1)}}{(k^2 - M_\pi^2)(k'^2 - M_\pi^2)} \right] \left[ \frac{[F_{\pi N}^+]^{(2)}}{(\tilde{k}^2 - M_\pi^2)(\tilde{k}'^2 - M_\pi^2)} \right] \end{aligned} \quad (11)$$

where  $k(\tilde{k})$  and  $k'(\tilde{k}') = k(\tilde{k}) + p' - p$  are the momenta of the exchanged pions,  $p(p')$  are relative  $NN$  momenta in the initial (final) state and the superscripts refer to nucleons (1) and (2), respectively.  $F_{\pi N}^+$  is the isospin symmetric part of the  $\pi N$  amplitude, Eq. (9), and the scalar-isoscalar tree level contact interaction  $V_{\pi\pi}^{L=I=0}$  is given by the Eq. (6). The diagrammatic representation of Eq. (11) is shown in Fig. 1.

The above expression, Eq. (11) has well known difficulties. It involves the off-mass-shell  $\pi\pi$  interaction which is not unique and depends on the choice of the interpolating pion field (parameterization of the  $SU(2)$  matrix  $U$ ) [15, 43]. If the initial and final pions are all on the mass shell, i.e.  $\Lambda_i = 0$  in Eq. (6), the  $\pi\pi$  scattering amplitude is independent of a change of field variables in agreement with the equivalence theorem [44]. In other words Eq. (6) gives a unique result independent of the parameterization of  $U$  only for the on-shell matrix elements. To avoid these ambiguities it was stated in Ref. [15] that one has to include a subset of diagrams to find cancellations of the off-shell  $\pi\pi$  isoscalar amplitude. This statement was rigorously verified in Ref. [26], where it was shown that the additional consideration of a subset of chiral diagrams results in exact cancellations of the off-shell part of the  $\pi\pi$  amplitude and the on-shell residue can be factorized out from the loop integrals of Eq. (11). By this and using notations of Ref. [42] the  $NN$  amplitude in the general

case of  $L = I = 0$   $\pi\pi$  exchange takes the form

$$\mathcal{V}_{NN}(t) = 6 [\Gamma_N^+(t)]^{(1)} [\Gamma_N^+(t)]^{(2)} \tilde{V}_{\pi\pi}^{L=I=0}(t), \quad (12)$$

where  $\tilde{V}_{\pi\pi}^{L=I=0}$  is the on-mass shell part of Eq. (6) with  $s \rightarrow t = (p' - p)^2 = -\mathbf{q}^2$  in the  $NN$  c.m. frame. In Eq. (12) the "vertex functions"  $[\Gamma_N^+(t)]$  are defined by

$$-i[\Gamma_N^+(t)]^{(i)} = -\frac{1}{2} \int \frac{d^4 k}{(2\pi)^4} \frac{[F_{\pi N}^+]^{(i)}}{(k^2 - M_\pi^2)(k'^2 - M_\pi^2)} \quad (13)$$

and can be interpreted in the heavy and relativistic baryon  $\chi$ PT as one-pion-loop contributions to the scalar form factor of the nucleon  $\sigma(t)$  [15, 45]:

$$[\Gamma_N^+(t)]^{(i)} = \frac{1}{3} \frac{\sigma(t)}{M_\pi^2} [\bar{u}u]^{(i)}. \quad (14)$$

At  $t = 0$  the  $\sigma(0)$  is referred to as the pion-nucleon sigma-term,  $\sigma_{\pi N}$ . Note, that by construction the factor  $\sim 1/M_\pi^2$  entering Eq. (14) is a direct reflection of the chiral symmetry breaking part of the  $\chi$ PT Lagrangian, Eq. (1). The resulting  $NN$  scattering amplitude can be summarized as follows

$$\mathcal{V}_{NN}(t) = \frac{2}{3} \left( \frac{\sigma(t)}{M_\pi^2} \right)^2 [\bar{u}u]^{(1)} [\bar{u}u]^{(2)} \tilde{V}_{\pi\pi}^{L=I=0}(t) \quad (15)$$

The quasi-potential reduction of the  $NN$  amplitude Eq. (15) is a standard procedure. The Partovi-Lomon method is the most popular one and allows to reduce the Bethe-Salpeter kernel to the quasi-potential containing minimal relativity [46]. The latter is ready for the iteration in the Lippmann-Schwinger equation. Here we follow Ref. [26] and wish to discuss the non-relativistic potential only. With the normalization for Dirac spinors,  $\bar{u}(p, s)u(p, s) = 1$ , the non-relativistic CrTPE potential is obtained from Eq. (15) simply by keeping its energy independent parts:

$$\mathcal{V}_{NN}(t) = \frac{2}{3} \left( \frac{\sigma(t)}{M_\pi^2} \right)^2 \tilde{V}_{\pi\pi}^{L=I=0}(t) \left[ 1 - \frac{\Omega_{LS}}{2M_N^2} \right]. \quad (16)$$

In square brackets the first term gives the central CrTPE potential  $\mathcal{V}_C(t)$ , with the structure similar to that derived in Ref. [15], and the second term provides the additional spin-orbit part  $\mathcal{V}_{LS}(t)$  with the spin content:  $\Omega_{LS} = i(\boldsymbol{\sigma}^{(1)} + \boldsymbol{\sigma}^{(2)})(\mathbf{p}' \times \mathbf{p})/2$ . In coordinate space the central potential is given by the Fourier transform of  $\mathcal{V}_C(t)$  and the spin-orbit ( $LS$ ) part of the  $NN$  force is related to the central potential simply by [46]

$$\mathcal{V}_{LS}(r) = -\frac{1}{2M_N^2} \frac{1}{r} \frac{\partial \mathcal{V}_C(r)}{\partial r}, \quad (17)$$

where the spin-orbit operator  $\hat{\Omega}_{LS}$  in  $r$ -space representation has been omitted. The central part of Eq. (16) has an interesting feature. Its long-range tail or the value of the potential at  $t = 0$  is

determined by the pion-nucleon sigma term:  $\mathcal{V}_C(0) = \sigma_{\pi N}^2 / 3M_\pi^2 f_\pi^2$ . So, the only unknown element which enters Eq. (16) is the scalar form factor of the nucleon. As noted in Refs. [42, 45] Eq. (14) and therefore also Eqs. (15) and (16) are general and should be independent of models or approximation schemes used to calculate the scalar form factor of the nucleon. In this work, we calculate  $\sigma(t)$  in the large- $N_c$  limit in the framework of the  $\chi$ QSM. But before doing model calculations the stated large- $N_c$  behavior of Eq. (16) must be understood and consistency with large- $N_c$  QCD analyses must be shown.

#### IV. LARGE- $N_c$ SCALING AND CONSISTENCY

In this section we explore qualitative features of the scalar-isoscalar components of the CrTPE force Eq. (16) which may be understood directly from QCD. In this context, it may be useful to consider the interaction in the limit, when the number of colors,  $N_c$ , of QCD becomes large [47, 48], and to treat  $1/N_c$  as an expansion parameter. Some features of the  $NN$  force can be obtained in this limit in a model-independent way [38, 49, 50]. Recently, it was realized that large- $N_c$  nuclear interactions are spin-flavor  $SU(4)$  symmetric, with Wigner's supermultiplet symmetry following as an accidental symmetry [49]. If we assume, in addition, that the spin-flavor symmetry properties of the  $NN$  interaction are independent of phases of the many body ground state (at  $N_c \rightarrow \infty$  nuclear matter forms a classical crystal, and a phase transition between  $N_c = 3$  and  $N_c = \infty$  is expected [38]), then the large- $N_c$  scaling behavior of the  $NN$  force can be analyzed in a general way resulting in QCD expectations which can explain general features of the  $NN$  interaction [38, 49].

The first treatment of the  $NN$  interaction in large- $N_c$  QCD was done in Ref. [48], where it was argued that the dominant interaction between two baryons is of order  $\sim \mathcal{O}(N_c)$ . This expectation is consistent with nuclear dynamics where the dominant interaction components are isoscalar-scalar and -vector interactions

$$\mathcal{V}_\sigma \sim \mathcal{O}(N_c), \quad \mathcal{V}_\omega \sim \mathcal{O}(N_c). \quad (18)$$

In phenomenological models, the latter can be parameterized in terms of effective  $\sigma$  and  $\omega$  exchanges [31]. The entire analysis of the  $NN$  potential was done in Ref. [38] where it was found that large- $N_c$  QCD implies that the scalar-isoscalar central and spin-orbit forces scale as

$$\mathcal{V}_C \sim \mathcal{O}(N_c), \quad \mathcal{V}_{LS} \sim \mathcal{O}(1/N_c). \quad (19)$$

Recently, the dynamical interpretation of the  $NN$  interaction for four modern phenomenologically successful models [27, 28, 29, 30] in the large- $N_c$  limit was reported and consistency of their scalar-isoscalar components with Eq. (19) was found [31].

In our case, the consistency condition implies that the large- $N_c$  scaling behavior of Eq. (16) must be consistent with large- $N_c$  QCD analysis [38], with the large- $N_c$  scaling of scalar-isoscalar components of all known phenomenologically successful  $NN$  interaction models [31] and also with effective  $\sigma$  meson exchange,  $\mathcal{V}_\sigma \sim \mathcal{O}(N_c)$ . The dynamical quantities which enter the scalar-isoscalar CrTPE force, Eq. (16), are the scalar form factor  $\sigma(t)$ , the pion mass  $M_\pi$ , the nucleon mass  $M_N$  and the  $\pi\pi$  scattering amplitude  $V_{\pi\pi}$  which scales as  $V_{\pi\pi} \sim \mathcal{O}(1/N_c)$ , Eq (7). We follow standard  $N_c$  counting rules [39, 51] where  $\sigma(t) \sim \mathcal{O}(N_c)$ ,  $M_\pi \sim \mathcal{O}(1)$ ,  $M_N \sim \mathcal{O}(N_c)$  and the nucleon momenta  $|\mathbf{p}|, |\mathbf{p}'| \sim \mathcal{O}(1)$ . Counting powers of  $N_c$  the central part of the CrTPE potential, first term in Eq. (16), is  $\mathcal{V}_C \sim \mathcal{O}(N_c)$ . Its spin-orbit counterpart  $\mathcal{V}_{LS}(t)$  additionally contains two inverse powers of nucleon mass  $\sim 1/M_N^2 \sim 1/N_c^2$  resulting in  $\mathcal{V}_{LS} \sim \mathcal{O}(1/N_c)$ . By this, the consistency with scaling relations from large- $N_c$  QCD Eq. (19) is noted. Interestingly, Eq. (19) implies that the spin-orbit force  $\mathcal{V}_{LS}$  is  $\mathcal{O}(1/N_c^2)$  in strength relative to the central force  $\mathcal{V}_C$  [38]

$$\mathcal{V}_{LS}/\mathcal{V}_C \sim \mathcal{O}(1/N_c^2) \quad (20)$$

We refer to Eq. (20) as the Kaplan-Manohar scaling relation [38]. In the last section it will be shown that Eq. (20) is very accurate and in remarkable agreement with our results, signaling that, indeed, with the actual number of colors  $N_c = 3$  the relative strength of potentials scales like  $\mathcal{V}_{LS}/\mathcal{V}_C \simeq 1/9$ .

## V. SCALAR FORM FACTOR IN THE LARGE- $N_c$ LIMIT AND QUARK-SOLITON MODEL

In the large- $N_c$  limit, the QCD is equivalent to an effective theory of mesons with baryons emerging as solitonic configurations [48]. The  $\chi$ QSM [36] provides a practical realization of the large- $N_c$  picture of the nucleon and is considered as a chiral relativistic quantum field theory of quarks, anti-quarks and Goldstone bosons. It is defined by the partition function in Euclidian space which is the path-integral over pseudoscalar meson and quark fields [52, 53]

$$\mathcal{Z} = \int \mathcal{D}\psi \mathcal{D}\bar{\psi} \mathcal{D}U \exp \left[ i \int d^4x \bar{\psi} (i \not{\partial} - M_q U^{\gamma_5} - m_q) \psi \right] \quad (21)$$

where  $U$  denotes the  $SU(2)$  pion field, Eq. (2),

$$U^{\gamma_5} = \exp(i\gamma_5\Phi/f_\pi) = \frac{1}{2}(U + U^\dagger) + \frac{1}{2}(U - U^\dagger)\gamma_5 \quad (22)$$

In Eq. (21)  $M_q$  and  $m_q$  are dynamical, arising from spontaneous breaking of chiral symmetry and current quark masses, respectively. The action, Eq. (21), was derived from the instanton vacuum model [52], where the cut-off is determined by the average size of instantons  $\langle\rho\rangle$ , and the dynamical quark mass  $M_q$  is momentum dependent. In the large- $N_c$  limit the chiral bosonic fields  $U^{\gamma_5}$  can be integrated out by the saddle point method using a classical background field of *hedgehog* shape

$$\boldsymbol{\pi}(\mathbf{x}) = f_\pi \hat{\mathbf{r}} \mathcal{P}(r) \quad (23)$$

which plays the role of a Hartree-type mean field for quarks forming a soliton-like bound state. With  $r = |\mathbf{x}|$  and  $\hat{\mathbf{r}} = \mathbf{x}/r$ , the variational procedure reduces to the determination of the self-consistent soliton profile  $\mathcal{P}(r)$ , where  $\mathcal{P}(r \rightarrow \infty) = 0$  and  $\mathcal{P}(0) = -\pi$  produce a soliton with unit winding number. In practical calculations the soliton size  $R_s = 1/M_q$  is treated as a free parameter, playing the role of the axial coupling constant  $g_A$  [36]

$$\lim_{r \rightarrow \infty} \left[ \lim_{m_\pi \rightarrow 0} r^2 \mathcal{P}(r) \right] = -2R_s^2 = -\frac{3}{8\pi} \frac{g_A}{f_\pi^2} \quad (24)$$

Nucleon states of definite spin and isospin are obtained by quantizing the rotational zero modes of the soliton.

The model expression for the scalar form factor of the nucleon in the  $\chi$ QSM is quadratically ultraviolet (UV) divergent and requires regularization [54, 55]

$$\sigma(t) = m_q N_c \int d^3 \mathbf{x} j_0(\sqrt{-t}|\mathbf{x}|) \sum_n \mathcal{D}_n(\mathbf{x}) \Big|_{\text{reg}} \quad (25)$$

Here  $\mathcal{D}_n(\mathbf{x}) = \Phi_n^*(\mathbf{x}) \gamma_0 \Phi_n(\mathbf{x})$  is the scalar-quark density in the nucleon and  $j_0$  is the spherical Bessel function. The completeness of quark Fock states  $|n\rangle$  in the external pion field require that  $\mathcal{D}_n$  is represented as a sum over occupied (valence) and non-occupied negative energy Dirac-sea states. So it is useful to consider the contributions from discrete levels (*lev*) and from the Dirac-sea (*sea*) continuum separately.  $\sigma_{\text{lev}}(t)$  is finite and requires the single-particle wave functions  $|\Phi_{\text{lev}}(\mathbf{x})\rangle$  to be found from the Dirac equation in the external pion field. The latter can be solved numerically.  $\sigma_{\text{sea}}(t)$  is UV divergent and depends on the regularization scheme employed to make it finite. To obtain  $\sigma_{\text{sea}}(t)$  we follow the method developed in Ref. [37]. In short, the procedure is as follows.

To evaluate  $\sigma_{sea}(t)$ , the model expression for the continuum contribution is expanded in a series of the  $U$ -field gradients - the interpolation formula method [56]. The series in  $\nabla U$  contains UV-divergent and UV-finite parts. As was shown in Ref. [37] the latter is strongly suppressed with respect to the UV-divergent term by the instanton packing fraction or parametric smallness of  $M_q^2 \langle \rho \rangle^2 \ll 1$ , and can be neglected. The dynamical quark mass is momentum independent and its value  $M_q = 350$  MeV is taken at zero momentum transfer from instanton phenomenology [57]. We recall that the  $\chi$ QSM is defined with some appropriate regularization. In Ref. [37] the regularization procedure is solved in a model independent way by observing that the structure of divergencies in  $\sigma_{sea}$  are the same as in model expressions for the vacuum scalar-quark condensate  $\langle \bar{\psi} \psi \rangle$  and pion decay constant  $f_\pi$ . The latter are fixed by their empirical values. The “arctan-profile” function which provides an accurate representation of the self-consistent profile is used

$$\mathcal{P}(r) = -2 \arctan \left[ \frac{R_s^2}{r^2} (1 + M_\pi r) e^{-M_\pi r} \right]. \quad (26)$$

Above steps result in a model expression for  $\sigma_{sea}(t)$ :

$$\sigma_{sea}(t) = M_\pi^2 f_\pi^2 \int_0^\infty d^3 \mathbf{r} j_0(r\sqrt{-t}) \left[ \frac{2\xi^2}{1 + \xi^2} \right], \quad (27)$$

where  $\xi = (R_s^2/r^2)(1 + M_\pi r)e^{-M_\pi r}$ . It follows that due to the partial cancellation of additional contributions from discrete levels and second order continuum terms in the  $\nabla U$  expansion, the accuracy of Eq. (27) in the limiting case  $\sigma_{sea}(t) \rightarrow \sigma(t)$  is  $\mathcal{O}(15\%)$ . The latter corresponds to the extreme case that the nucleon scalar quark density is formed exclusively by the Dirac-sea (pion cloud). With the expected accuracy Eq. (27) reproduces all features of the scalar form factor observed in exact  $\chi$ QSM calculations and also in  $\chi$ PT and compares well to lattice QCD results. Eq. (27) results in pion-nucleon sigma term  $\sigma_{\pi N} = \sigma(0) \simeq 68$  MeV, which is consistent with empirical information [58, 59]. The analytical simplicity of Eq. (27) is a big advantage of this method. We refer to Ref. [37] for details and use Eq. (27) for our numerical calculations. In addition, consider the pion mass expansion of the profile function  $\mathcal{P}(r)$ , Eq. (26)

$$\mathcal{P}(r, M_\pi) = -2 \arctan \left( \frac{R_s^2}{r^2} \right) + \mathcal{O}(M_\pi^2). \quad (28)$$

In the  $\chi$ QSM the soft pion limit,  $\mathcal{P}(r, M_\pi \rightarrow 0)$ , is known to approximate well both the self-consistent profile and Eq. (26). Following the method of Ref. [37], we find that in this limit  $\sigma(t)$  takes an even simpler form

$$\sigma(t) = \frac{4\pi^2}{\sqrt{2}} M_\pi^2 f_\pi^2 R_s^3 j_0(R_s \sqrt{-t/2}) e^{-R_s \sqrt{-t/2}}. \quad (29)$$

If one would expand Eq. (27) in Taylor series around  $M_\pi = 0$ , then Eq. (29) corresponds to the leading analytic  $\sim M_\pi^2$  contribution to the scalar form factor or to the  $\pi N$  sigma term,  $\sigma_{\pi N}$ , defined by Eq. (27). The quality of this representation will be discussed later. We only note that, a simple form of Eq. (29) is very successful, at least for our considerations, because it allows us to express all our final results for the  $r$ -space CrTPE potential in terms of elementary functions. Furthermore, Eq. (29) accounts for all details of the CrTPE force observed here and compares well with direct numerical calculation obtained with Eq. (27).

## VI. RESULTS AND DISCUSSION

### A. The central CrTPE force: tree-level *vs* unitary $\pi\pi$ scattering amplitude

In the discussion of our results we start from the scalar-isoscalar central  $NN$  potential in coordinate space, which is given by the Fourier transform of the first term in Eq. (16). Our results for  $\mathcal{V}_C(r)$  with the scalar form factor  $\sigma(t)$  defined by Eq. (27) and the tree level  $\pi\pi$  correlation function, Eq. (6), are shown in Fig. 2 (dashed curve). The central potential  $\mathcal{V}_C(r)$  shows a short-range repulsive core with a maximum at the origin,  $\mathcal{V}_C(r = 0) \simeq 600$  MeV (see insert of Fig. 2), and is supplemented by a moderate attraction with a minimum,  $\mathcal{V}_C \simeq -20$  MeV, at intermediate distances  $r > 1$  fm. This behavior is different from the conventional picture provided by the effective  $\sigma$  exchange in OBE models and also from results obtained in the heavy baryon  $\chi$ PT [15]. In Ref. [15] the effect of the CrTPE in the scalar-isoscalar channel is very weak and repulsive. The latter means, that the  $t$ -dependence of the vertex functions or functional form of the scalar form factor is very important for determining the precise strength and behavior of the potential in all ranges of distances. At the same time one can find a remarkable agreement between our results and the analysis of Ref. [26], where the unitary  $\pi\pi$  amplitude Eq. (30) has been coupled to the nucleon cloud at the one pion loop. In Ref. [26] the divergent loop-integrals were regulated by phenomenological vertex form factors. Being sensitive to the particular choice of the cut-off mass, the resulting scalar-isoscalar central  $NN$  potential shows a strong repulsion at internucleon distances less than 1 fm, and a moderate attraction of  $-10(-15)$  MeV, at  $r > 1$  fm.

To make our results comparable with that from Ref. [26] we unitarize the  $\pi\pi$  scattering ampli-

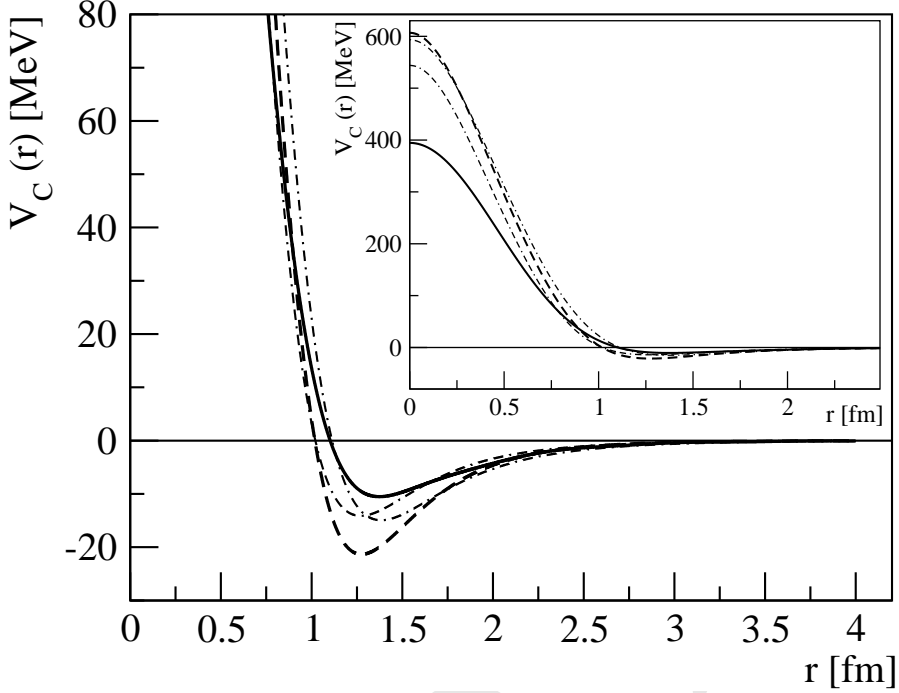


FIG. 2: The central CrTPE potential in coordinate space obtained with tree level (dashed curve) and unitarized (solid curve)  $\pi\pi$  scattering amplitude. The dot-dashed and dash-dash-dotted curves correspond to the soft pion limit with  $M_q = 350$  MeV and  $M_q = 410$  MeV, respectively. The insert shows the entire structure of the  $NN$  potential.

tude, Fig. 3. It can be done by the following substitution [25]

$$\tilde{V}_{\pi\pi}^{L=I=0} = - \left[ f_\pi^2 \left( s - \frac{M_\pi^2}{2} \right)^{-1} + G_{\pi\pi}(s) \right]^{-1}, \quad (30)$$

where  $G_{\pi\pi}(s)$  is a dimensionally regularized two-pion loop function (see e.g. Ref. [26])

$$G_{\pi\pi}(s) = \frac{1}{(4\pi)^2} \left[ -1 + \ln \frac{M_\pi^2}{\mu^2} + \sigma \ln \frac{\sigma + 1}{\sigma - 1} \right]. \quad (31)$$

Here  $\mu = 1.1$  GeV is the regularization mass fitted to the  $\pi\pi$  phase shifts. The value of  $\sigma$  in Eq. (31) is given by  $\sigma = \sqrt{1 - \frac{4M_\pi^2}{s}}$ . Eq. (31) is analytic in space-like and time-like regions and for  $s > 4M_\pi^2$  it develops an imaginary part, since  $\sigma - 1 < 0$  and  $\ln \frac{\sigma + 1}{\sigma - 1} = \ln \frac{\sigma + 1}{1 - \sigma} + i\pi$ . For  $s \rightarrow t < 0$  the log behaves smoothly. Because Eq. (30) contains a pole in the  $s$ -channel around  $M_{\pi\pi} - i\Gamma/2 \simeq 450 - i221$  MeV, we restore the genuine relation to the  $\sigma$ -meson exchange, which now enters in our formalism as dynamical resonance in the  $\pi\pi$  system. The main effect of the unitary  $\pi\pi$  scattering amplitude ( $\sigma$  meson) in the  $t$ -channel is that it makes the repulsion  $\simeq 400$  MeV and attraction  $\simeq -10$  MeV softer (solid curve in Fig. 2). However it does not change the general

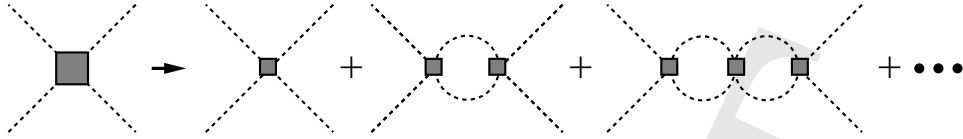


FIG. 3: Unitarization of the  $\pi\pi$  scattering amplitude.

features of the  $NN$  force already obtained at tree level. Interestingly, the latter effect is opposite to the role played by the the unitarization in the  $s$ -channel, where it leads to an enhancement of the interaction strength between pions.

Another point is the relation of the effective  $\sigma$  meson exchange of OBE models to the unitary scalar-isoscalar CrTPE force constructed here. In Ref. [31] the volume integrals were used to extract the strength of scalar-isoscalar components of phenomenological  $NN$  models and to relate them to the effective  $\sigma$  exchange. It was shown that if the mass of the  $\sigma$  is taken to be  $M_\sigma = 600$  MeV then the value of the  $\sigma NN$  coupling constant for these interactions would range between  $g_{\sigma NN} = 7.6$  (Paris), 9.0 (Argonne V18), 9.8 (Nijmegen) and 11.2 (CD-Bonn). It follows from Ref. [26], that the use of the unitary  $\pi\pi$  scattering amplitude Eq. (30) results in an effective  $\sigma NN$  coupling constant which can be expressed as

$$g_{\sigma NN} \simeq \sqrt{6} V(t=0) (M_\sigma^2 - M_\pi^2/2) / f_\pi. \quad (32)$$

Here,  $V(t)$  is a vertex function which accounts for the coupling of the  $\pi\pi$  correlation function to the nucleon pion cloud, and  $M_\sigma$  is an empirical  $\sigma$  meson mass. Note that the use of  $M_\sigma = 600$  MeV in this case is not entirely correct, because this value does not represent the actual pole of Eq. (30). With the quoted value of  $V(t)$  at  $t = 0$  [26]:  $V(0) \simeq 0.1 \times 10^{-2}$  MeV $^{-1}$  and the  $\sigma$  mass (pole)  $M_\sigma \simeq 450$  MeV the resulting coupling is  $g_{\sigma NN} \simeq 5$ , which has the right order of magnitude. In our case, note that the vertex function  $V(t)$  as provided by Ref. [26] is equivalent to our  $\Gamma_N^+(t) = V(t)$  in Eq. (12). By this, we rewrite Eq. (32) and relate the  $\sigma NN$  coupling constant to the  $\pi N$  sigma term  $\sigma_{\pi N}$

$$g_{\sigma NN} \simeq \sqrt{\frac{2}{3}} \sigma_{\pi N} (M_\sigma^2 - M_\pi^2/2) / (f_\pi M_\pi^2). \quad (33)$$

Eq. (27) results in  $\sigma_{\pi N} \simeq 68$  MeV and our value for the  $V(t = 0)$  is given by:  $V \simeq 0.12 \times 10^{-2}$  MeV $^{-1}$ . With  $M_\sigma = 450$  MeV our result is  $g_{\sigma NN} \simeq 6.1$ . An artificial increase of the  $\sigma$  mass to  $M_\sigma = 600$  MeV, used in analysis of Ref. [31], results in  $g_{\sigma NN} \simeq 11$  which is just in the range of values from phenomenological models [31].

Using the equivalence between  $\Gamma_N^+(t)$  and  $V(t)$  we independently verify the theoretical consistency of Ref. [26]. Indeed, with  $V(0)$  obtained in Ref. [26] the resulting  $\pi N$  sigma term is  $\sigma_{\pi N} \simeq 57$  MeV and is within the range of empirical values [58, 59]. It means that values of cut-off masses used in Ref. [26] are reasonable and consistent with our results and with empirical information. There is also consistency between the large- $N_c$  behavior of Eq. (33) and large- $N_c$  QCD expectations, where a scalar-meson  $NN$  coupling constant is  $\sim \mathcal{O}(\sqrt{N_c})$  [38]. Because the  $1/N_c$  expansion of the  $\pi N$  sigma term follows the large- $N_c$  behavior of the scalar form factor  $\sigma_{\pi N} \sim \mathcal{O}(N_c)$ , the pion decay constant  $f_\pi \sim \mathcal{O}(1/\sqrt{N_c})$ ,  $M_\pi \sim \mathcal{O}(1)$  and  $M_\sigma \sim \mathcal{O}(1)$  [60] we get

$$g_{\sigma NN} \sim \mathcal{O}(\sqrt{N_c}), \quad (34)$$

in agreement with large- $N_c$  counting rules [38].

The noncommutativity of large- $N_c$  and chiral limits is a well-known phenomenon [61]. The important physics behind this is the role of the  $\Delta(1232)$  isobar. In the large- $N_c$  limit nucleon and  $\Delta$  are degenerate with mass difference  $M_\Delta - M_N \sim \mathcal{O}(1/N_c)$ . As a consequence the contribution of  $\Delta$  states is implicitly included in solitonic configurations and their effect on scalar-isoscalar quantities is twice that of nucleon states [37, 62]. Note that, therefore the leading non-analytic contribution to  $\sigma_{\pi N}$ , which is  $27g_A^2 M_\pi^3/(64\pi f_\pi^2)$  obtained by expanding Eq. (27), is exactly three times larger than the corresponding value in  $\chi$ PT including nucleons and pions only. Being common for generic classes of hedgehog models [62], this result can be explained by the presence of the intermediate  $\Delta$  states in chiral loops. If one goes beyond the strict large- $N_c$  limit the effect of finite  $N - \Delta$  mass splitting must be taken into account, the magnitudes of the resulting corrections are known [62].

## B. Saturation of the LEC $c_1$

Here we use constraints imposed by chiral symmetry to check the consistency of the present approach. Consider the LEC  $c_1$  from  $\chi$ PT which is related to the  $\pi N$  sigma term  $\sigma_{\pi N}$  [16]. The phenomenological interpretation of its value is based on the strongly coupled scalar-isoscalar meson exchange which can completely saturate  $c_1$ , if [17]

$$\frac{M_\sigma}{\sqrt{g_{\sigma NN}}} = 180 \text{ MeV.} \quad (35)$$

It is interesting to note that the effective  $\sigma$  meson in the Bonn potential [4] with  $M_\sigma = 550$  MeV and  $g_{\sigma NN}^2/(4\pi) = 7.1$  respects this condition resulting in  $M_\sigma/\sqrt{g_{\sigma NN}} \simeq 179$  MeV. In our case,

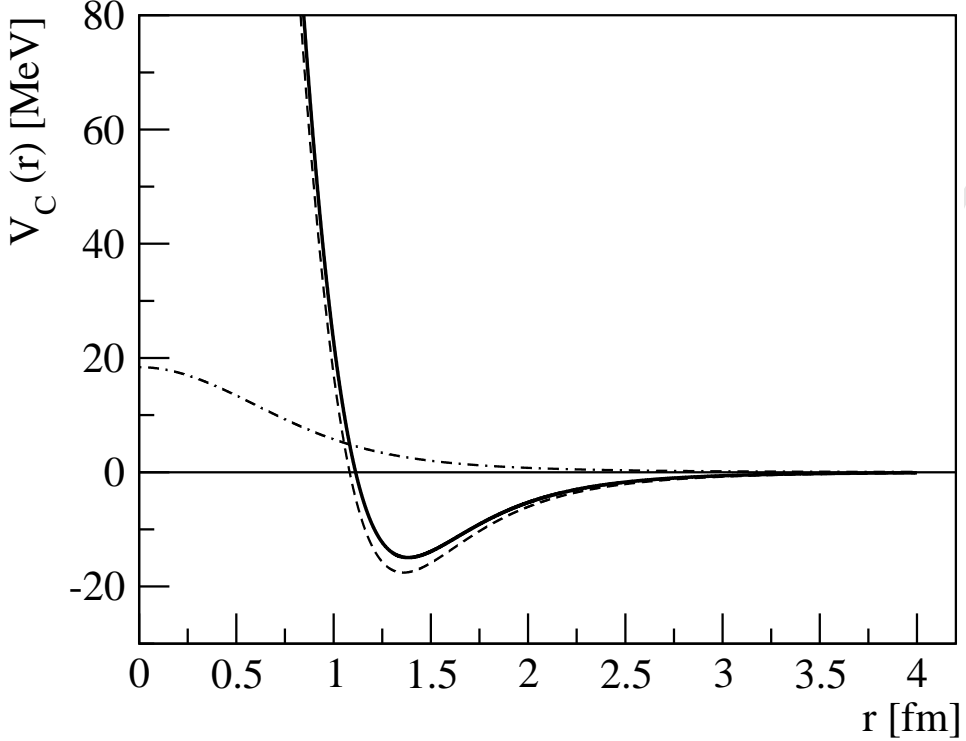


FIG. 4: The central CrTPE potential in the soft pion limit (solid curve). The parts non-vanishing and vanishing in the chiral limit are shown by the dashed and dot-dashed curves, respectively.

using the pole of Eq. (30), i.e.  $M_\sigma = 450$  MeV, and  $g_{\sigma NN} = 6.1$ , Eq. (33), the saturation condition is

$$\frac{M_\sigma}{\sqrt{g_{\sigma NN}}} \simeq 182 \text{ MeV.} \quad (36)$$

which is in agreement with the value demanded from the scalar meson resonance saturation of the LEC  $c_1$ .

### C. Analytical formulae for the central force

The consideration of the central part can be continued in the soft pion limit where  $\sigma(t)$  is given by Eq. (29). In this case the central CrTPE force in the coordinate space representation can be expressed in terms of elementary functions. First, decompose the tree level  $\pi\pi$  correlation function defined by Eq. (6) into two terms,  $\tilde{V}_{\pi\pi}^{L=I=0} = \tilde{V}_{\pi\pi}^{(1)} + \tilde{V}_{\pi\pi}^{(2)}$ :

$$\tilde{V}_{\pi\pi}^{(1)} = -t/f_\pi^2, \quad \tilde{V}_{\pi\pi}^{(2)} = M_\pi^2/2f_\pi^2. \quad (37)$$

By this, the CrTPE force reads as

$$\mathcal{V}_{NN}(t) = \mathcal{V}_{NN}^{(1)}(t) + \mathcal{V}_{NN}^{(2)}(t). \quad (38)$$

In the soft pion limit, due to the factor  $1/M_\pi^2$  entering Eq. (16), the first term  $\mathcal{V}_{NN}^{(1)}$  does not contain any pion mass dependence and does not vanish in the chiral limit (non-vanishing part). The second term  $\mathcal{V}_{NN}^{(2)}$  which follows  $\tilde{V}_{\pi\pi}^{(2)}$  and contains an additional  $M_\pi^2$  generates the symmetry breaking part of the  $NN$  force. With Eqs. (29) and (37) the Fourier transform of Eq. (38) can be carried out explicitly and after lengthy calculations (here we list our final results only) the central CrTPE force is given in coordinate space by following expressions

$$\begin{aligned} \mathcal{V}_C^{(1)}(r) &= \left( \frac{64\sqrt{2}\pi^2}{3} \right) f_\pi^2 R_s \\ &\times \left[ \frac{80 + 8\tilde{\xi} + 3\tilde{\xi}^2 - 3\tilde{\xi}^3}{\left(2 + \tilde{\xi}\right)^2 \left(4 + \tilde{\xi} + 2\sqrt{2\tilde{\xi}}\right)^2 \left(4 + \tilde{\xi} - 2\sqrt{2\tilde{\xi}}\right)^2} \right] \end{aligned} \quad (39)$$

$$\begin{aligned} \mathcal{V}_C^{(2)}(r, \tilde{\xi} \leq 4) &= \frac{M_\pi^2}{r} \left( \frac{4\pi^2}{3} \right) f_\pi^2 R_s^4 \\ &\times \left[ \arctan \left( \sqrt{\frac{\tilde{\xi}}{2}} \right) - \frac{1}{2} \arctan \left( \frac{2\sqrt{2\tilde{\xi}}}{4 - \tilde{\xi}} \right) \right] \end{aligned} \quad (40)$$

$$\begin{aligned} \mathcal{V}_C^{(2)}(r, \tilde{\xi} > 4) &= \frac{M_\pi^2}{r} \left( \frac{4\pi^2}{3} \right) f_\pi^2 R_s^4 \\ &\times \left[ \arctan \left( \sqrt{\frac{\tilde{\xi}}{2}} \right) - \frac{1}{2} \left\{ \pi - \arctan \left( \frac{2\sqrt{2\tilde{\xi}}}{\tilde{\xi} - 4} \right) \right\} \right] \end{aligned} \quad (41)$$

where  $\tilde{\xi} = r^2/R_s^2$  and the superscripts (1) and (2) refer to the non-vanishing part and the symmetry breaking part, respectively. Note that Eqs. (40) and (41) are defined for  $\tilde{\xi} \leq 4$  and  $\tilde{\xi} > 4$ , respectively.

At small separation scales Eqs. (39) and (40) can be expanded in Taylor series around  $r \rightarrow 0$ , and up to  $\mathcal{O}(r^4)$  the leading terms are given by:

$$\mathcal{V}_C^{(1)}(r) \Big|_{r \rightarrow 0} = \frac{5\sqrt{2}\pi^2}{3} f_\pi^2 R_s - \frac{3\pi^2}{\sqrt{2}} \frac{f_\pi^2}{R_s} r^2 + \mathcal{O}(r^4), \quad (42)$$

$$\begin{aligned} \mathcal{V}_C^{(2)}(r) \Big|_{r \rightarrow 0} &= \frac{\sqrt{2}\pi^2}{3} f_\pi^2 M_\pi^2 R_s^3 \\ &- \frac{5\sqrt{2}\pi^2}{36} f_\pi^2 M_\pi^2 R_s r^2 + \mathcal{O}(r^4). \end{aligned} \quad (43)$$

The strength of the central force is defined by the sum of Eqs. (42) and (43) at  $r = 0$ :  $\mathcal{V}_C(0) = \mathcal{V}_C^{(1)}(0) + \mathcal{V}_C^{(2)}(0)$

$$\mathcal{V}_C(r) \Big|_{r=0} = \frac{5\sqrt{2}\pi^2}{3} \left( 1 + \frac{1}{5} M_\pi^2 R_s^2 \right) f_\pi^2 R_s. \quad (44)$$

For asymptotically large  $r \rightarrow \infty$  (up to  $\mathcal{O}(r^{-8})$ ) the interaction is dominated by molecular-like  $NN$  forces

$$\mathcal{V}_C^{(1)}(r) \Big|_{r \rightarrow \infty} = -64\sqrt{2}\pi^2 f_\pi^2 R_s^7 \frac{1}{r^6} + \mathcal{O}(r^{-8}), \quad (45)$$

$$\begin{aligned} \mathcal{V}_C^{(2)}(r) \Big|_{r \rightarrow \infty} &= \frac{8\sqrt{2}\pi^2}{3} M_\pi^2 f_\pi^2 R_s^7 \frac{1}{r^4} \\ &\quad - \frac{16\sqrt{2}\pi^2}{3} M_\pi^2 f_\pi^2 R_s^9 \frac{1}{r^6} + \mathcal{O}(r^{-8}). \end{aligned} \quad (46)$$

As seen from above expressions,  $\mathcal{V}_C^{(1)}$  and  $\mathcal{V}_C^{(2)}$  do not vanish at small separations and both are repulsive. At asymptotically large  $r$   $\mathcal{V}_C^{(1)}$  becomes attractive, signaling that it should cross the zero. Contrary, the symmetry breaking part,  $\mathcal{V}_C^{(2)}$ , stays repulsive for all distances and as a result of  $\mathcal{V}_C^{(2)}/\mathcal{V}_C^{(1)} \sim M_\pi^2 R_s^2/5 \ll 1$  it is suppressed relative to  $\mathcal{V}_C^{(1)}$ . The above qualitative arguments are supported by full analytical representations given by Eqs. (39-41). The resulting central  $NN$  potential is shown in Fig. 4. It is clear from Fig. 4 that the part  $\mathcal{V}_C^{(1)}(r)$ , which is non-vanishing in the chiral limit (dashed curve), is dominant and fully drives the generic behavior of the central CrTPE force (solid line). The chiral part  $\mathcal{V}_C^{(2)}(r)$ , which is vanishing in the chiral limit (dot-dashed curve), is repulsive for all distances with a strength of about  $\simeq 20$  MeV at  $r = 0$ . Comparison with numerical results from the previous section reveals that at intermediate distances (dip region) the total CrTPE force obtained in the soft pion limit (shown by the dot-dashed curve in Fig. 2) lies in-between the tree level and unitarized curves. At small separation scales (see insert of Fig. 2) the integral Eq. (27) and analytical Eq. (29) representations for the scalar form factor work equally well, and the analytical and numerical tree level results are very close to each other.

Up to now, we used the common value of the dynamical quark mass  $M_q = 350$  MeV motivated by the instanton phenomenology. We have to mention that with this value the representation of  $\sigma(t)$  Eq. (29) overestimates the value of the  $\pi N$  sigma term obtained with Eq. (27) and the latter can be reproduced by a small variation of  $M_q$ . Note that, in the  $\chi$ QSM the dynamical quark mass is usually treated as a free parameter varying in the range  $350 < M_q < 450$  MeV. So it is important to check whether our results are sensitive to the variation of  $M_q$ . Certainly, due to Eq. (44) and the

parametric smallness of the term  $M_\pi^2 R_s^2/5 \ll 1$  the strength of the repulsive core is proportional to  $\sim 1/M_q$ . Interestingly, the strength of the intermediate range attraction actually is insensitive to variations of quark mass. In Fig. 2 we show the results for  $M_q \simeq 410$  MeV (dash-dash-dotted curve) which reproduces the same value of the sigma term  $\sigma_{\pi N}$  as Eq. (27) with  $M_q = 350$  MeV. The dip region is unaffected by these variations with a small coherent shift towards shorter distances. The same weak quark mass dependence is found in numerical calculations. Summarizing, the soft pion limit provides an accurate representation of the central CrTPE force, compares well with direct numerical calculations and accounts for all details of the tree level and unitary forces obtained in the previous section.

#### D. The spin-orbit CrTPE force

In coordinate space the spin-orbit part of the scalar-isoscalar CrTPE force is related to the central potential by Eq. (17). According to the large- $N_c$  analysis given in section IV, the  $LS$  interaction should be much smaller than the central part because it is suppressed relative to  $\mathcal{V}_C(t)$  by  $\sim 1/N_c^2$ . Our numerical results for the  $LS$  potential are shown in Fig. 5. Indeed, the  $r$ -space behavior of  $\mathcal{V}_{LS}(r)$  with the tree level  $\pi\pi$  scattering amplitude (dashed curve in Fig. 5) is formally similar to the central potential (see the insert of Fig. 2). But contrary to the  $\mathcal{V}_C(r)$ , we find a sizable but much weaker repulsive core  $\simeq 80$  MeV (insert of Fig. 5) and a very small attraction  $\simeq 0.5$  MeV at intermediate distances  $r > 1.2$  fm. The effect of the unitarization of the  $\pi\pi$  scattering amplitude (solid curve in Fig. 5) plays here the same role as for the central potential and makes the  $LS$  force softer reducing the strength of the potential by the factor two. Note, that in OBE models, the  $LS$  interaction induced by effective  $\sigma$  exchange generates an attractive spin-orbit force. In our case the effect is opposite and leads to a repulsive  $LS$  potential in coordinate space. In Ref. [26] the spin-orbit potential was not calculated (though it could be easily done) and hence direct comparison is not possible. We only note, that the results should be similar because of Eq. (17) and because of the similar behavior of  $\mathcal{V}_C(r)$  in both approaches.

At this level the comparison with other models is also useful. For example, in the standard Skyrme model [32], which includes the non-linear  $\sigma$  model Eq. (1) and a stabilizing fourth-order term, the “wrong sign” of the isospin independent spin-orbit potential is a long standing problem [63, 64]. Several attempts have already been done in this framework to generate the needed

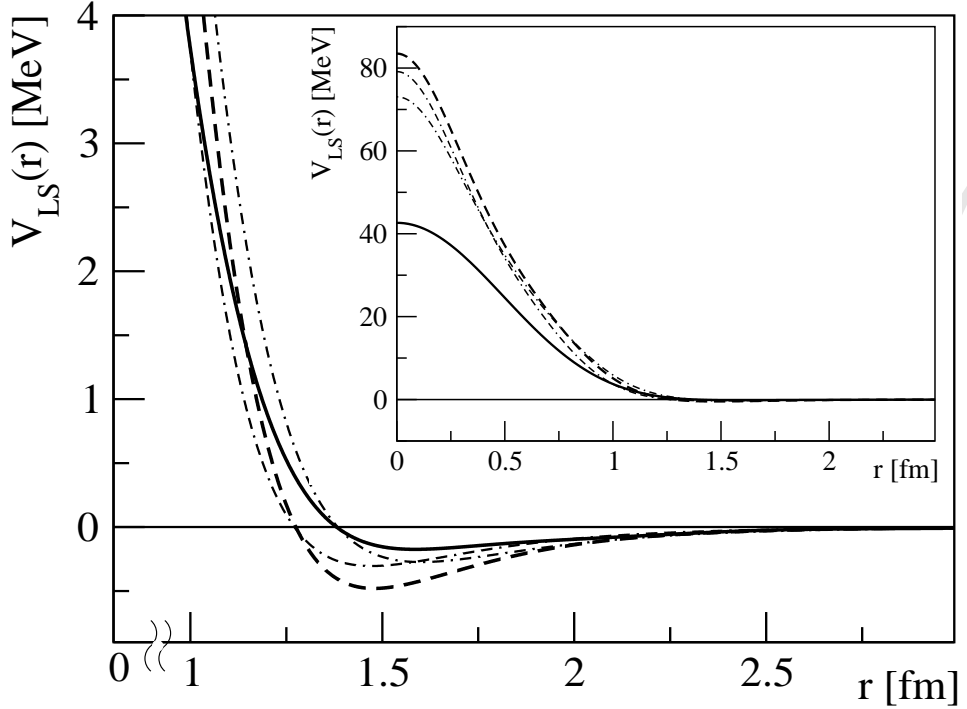


FIG. 5: The spin-orbit part of the CrTPE potential in coordinate space. Notations for the curves are the same as in Fig. 2. The insert shows the entire structure of the  $LS$  potential.

attractive spin-orbit force, extending the standard Skyrme Lagrangian by including sixth-order derivative terms. But the final results differ, varying from repulsive [64] to attractive [65] spin-orbit potential. Our results support the existence of a repulsive  $LS$  interaction in the isoscalar channel.

### E. Analytical formulae for the spin-orbit force

Here we show an analytical representation of the spin-orbit potential in coordinate space in terms of elementary functions. Using Eqs. (17) and (39), the  $LS$  part  $\mathcal{V}_{LS}^{(1)}$ , which is non-vanishing in the chiral limit, reads

$$\begin{aligned} \mathcal{V}_{LS}^{(1)}(r) = & \left( \frac{64 \sqrt{2} \pi^2}{3} \right) \frac{f_\pi^2}{R_s M_N^2} \\ & \times \left[ \frac{2304 + 576 \tilde{\xi} + 816 \tilde{\xi}^2 + 100 \tilde{\xi}^3 - 6 \tilde{\xi}^4 - 9 \tilde{\xi}^5}{\left( 2 + \tilde{\xi} \right)^3 \left( 4 + \tilde{\xi} + 2 \sqrt{2 \tilde{\xi}} \right)^3 \left( 4 + \tilde{\xi} - 2 \sqrt{2 \tilde{\xi}} \right)^3} \right] \end{aligned} \quad (47)$$

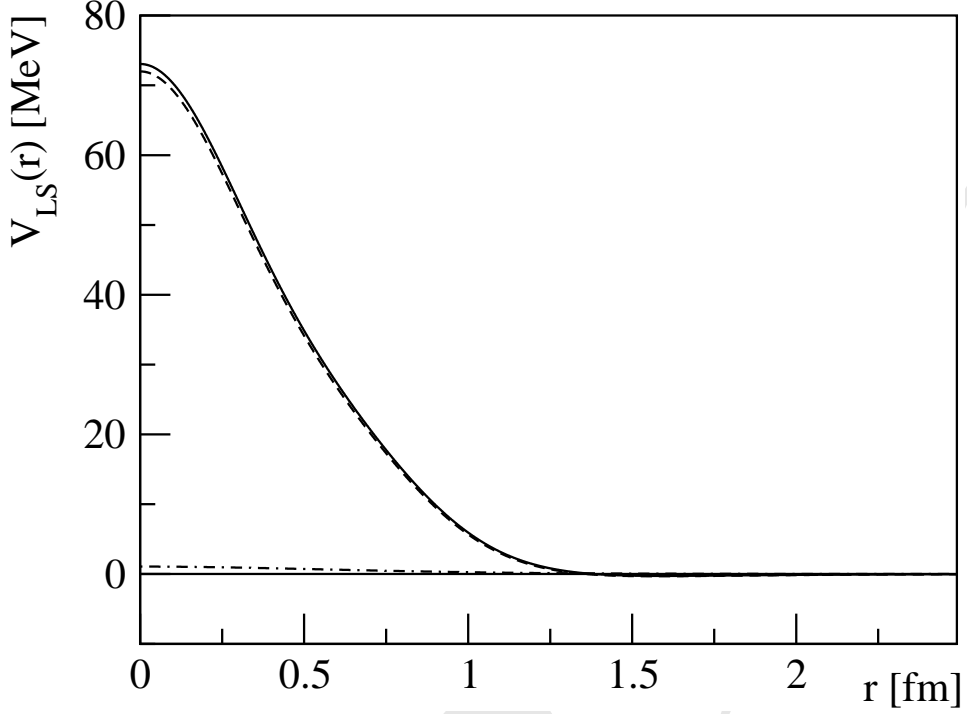


FIG. 6: The spin-orbit part of the CrTPE potential in the soft pion limit. Notations for the curves are the same as in Fig. 4.

Its symmetry breaking counterpart  $\mathcal{V}_{LS}^{(2)}$  vanishes in the chiral limit,  $M_\pi \rightarrow 0$ , and is obtained simply from Eqs. (17), (40) and (41)

$$\begin{aligned} \mathcal{V}_{LS}^{(2)}(r) &= \frac{1}{2M_N^2} \frac{1}{r^2} \mathcal{V}_C^{(2)}(r) \\ &\quad - \frac{M_\pi^2}{r^2} \left( \frac{4\sqrt{2}\pi^2}{3} \right) \frac{f_\pi^2 R_s^3}{M_N^2} \left[ \frac{4 - 3\tilde{\xi}}{(16 + \tilde{\xi}^2)(2 + \tilde{\xi})} \right] \end{aligned} \quad (48)$$

where for  $\tilde{\xi} = r^2/R_s^2 \leq 4$  and  $\tilde{\xi} > 4$  the  $\mathcal{V}_C^{(2)}(r)$  is given by Eqs. (40) and (41), respectively. The Taylor expansion around  $r \rightarrow 0$  up to  $\mathcal{O}(r^4)$  reads

$$\begin{aligned} \mathcal{V}_{LS}^{(1)}(r) \Big|_{r \rightarrow 0} &= \frac{3\pi^2}{\sqrt{2}} \frac{f_\pi^2}{R_s M_N^2} \\ &\quad - \frac{15\sqrt{2}\pi^2}{8} \frac{f_\pi^2}{R_s^3 M_N^2} r^2 + \mathcal{O}(r^4), \end{aligned} \quad (49)$$

$$\begin{aligned} \mathcal{V}_{LS}^{(2)}(r) \Big|_{r \rightarrow 0} &= \frac{5\sqrt{2}\pi^2}{36} f_\pi^2 R_s \frac{M_\pi^2}{M_N^2} \\ &\quad - \frac{3\sqrt{2}\pi^2}{40} f_\pi^2 \frac{1}{R_s} \frac{M_\pi^2}{M_N^2} r^2 + \mathcal{O}(r^4), \end{aligned} \quad (50)$$

and defines the short-range behavior of the  $LS$  force with the total strength at origin

$$\mathcal{V}_{LS}(r) \Big|_{r \rightarrow 0} = \frac{5\sqrt{2}\pi^2}{3} \left( \frac{9}{10} + \frac{1}{12} M_\pi^2 R_s^2 \right) \frac{f_\pi^2}{R_s M_N^2}. \quad (51)$$

In the asymptotic region,  $r \rightarrow \infty$ , the soft two-pion tail of the  $LS$  potential behaves as follows

$$\mathcal{V}_{LS}^{(1)}(r) \Big|_{r \rightarrow \infty} = -192 \frac{\sqrt{2}\pi^2}{M_N^2} f_\pi^2 R_s^7 \frac{1}{r^8} + \mathcal{O}(r^{-10}) \quad (52)$$

$$\mathcal{V}_{LS}^{(2)}(r) \Big|_{r \rightarrow \infty} = \frac{16\sqrt{2}\pi^2}{3} f_\pi^2 R_s^7 \frac{M_\pi^2}{M_N^2} \frac{1}{r^6} + \mathcal{O}(r^{-8}) \quad (53)$$

The result of Eqs. (47) and (48) with the quark mass  $M_q = 350$  MeV are shown in Fig. 6. The soft pion limit well reproduces the generic features of the  $LS$  force (solid line) and compares well with our numerical results (dot-dashed curve in Fig. 5). Contrary to the central force, even smaller contribution of the chiral part  $\mathcal{V}_{LS}^{(2)}(r)$  (dot-dashed curve in Fig. 6) with repulsive strength at  $r = 0$  of about  $\simeq 0.11$  MeV is noted. The term  $\mathcal{V}_{LS}^{(1)}(r)$  non-vanishing in the chiral limit accurately represents the behavior of the  $LS$  potential in all ranges of distances and is actually insensitive to the variation of quark masses in the intermediate region. The increase of the quark mass to  $M_q = 410$  MeV leads to a small shift of the attractive dip towards shorter distances (dash-dash-dotted curve in Fig. 5). At short separation scales, Eq. (51),  $M_\pi^2 R_s^2 / 12 \ll 1$  and the effect of quark mass is linear  $\sim M_q$  and opposite to the central force where the strength is driven by  $\sim 1/M_q$ .

## F. The ratio $V_{LS}/V_C$ and large- $N_c$ QCD scaling

According to large- $N_c$  counting rules discussed in section IV and Eq. (20), one can expect that with the actual number of colors  $N_c = 3$  the ratio  $V_{LS}/V_C$  should scale according to the following simple relation

$$\mathcal{V}_{LS}/\mathcal{V}_C \sim \mathcal{O}(1/N_c^2) = \mathcal{O}(1/9) \simeq 0.11 \quad (54)$$

Our results support these expectations and Eq. (54) for the relative strength of scalar-isoscalar  $NN$  components,  $\mathcal{R} = \mathcal{V}_{LS}(0)/\mathcal{V}_C(0)$ , is in a good agreement with numerical calculations. With  $\sigma(t)$  defined by Eq. (27) and with the tree level  $\pi\pi$  correlation function the ratio is:  $\mathcal{R} \simeq 1/7.26 \simeq 1.14$ . The unitarization of the  $\pi\pi$  scattering amplitude, Eq. (30), plays here an important role and improves this value to  $\mathcal{R} \simeq 1/9.2 \simeq 0.11$ . Considering the latter value as our parameter free prediction, it is remarkable that such detailed information about the relative strength of potential components can be deduced directly from QCD. Note that the  $1/N_c$  expansion is equivalent to

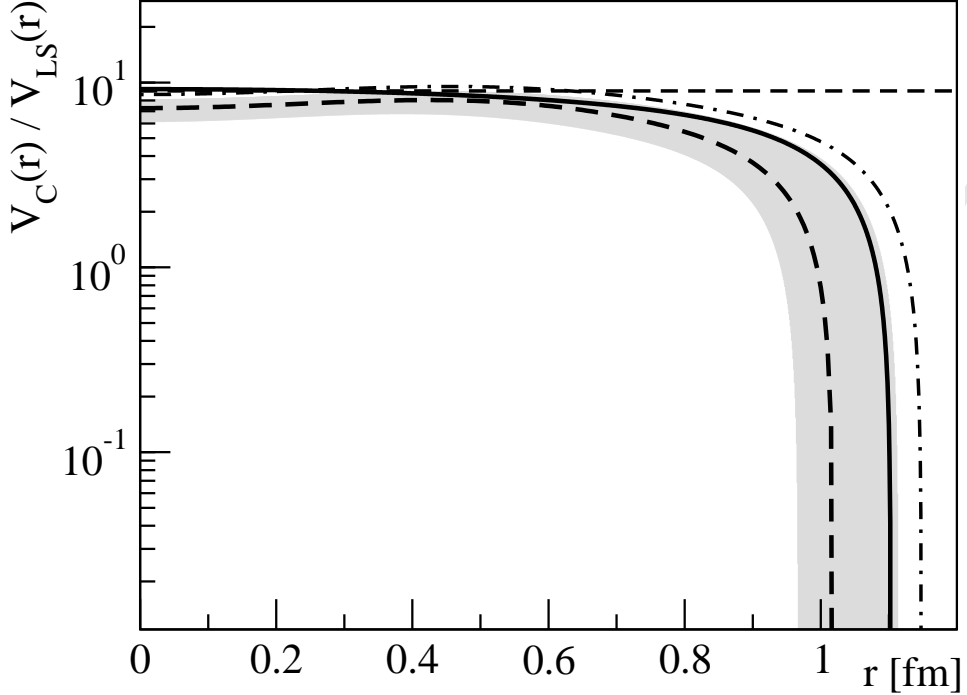


FIG. 7: The scaling of the central CrTPE force  $\mathcal{V}_C(r)$  relative to the spin-orbit potential  $\mathcal{V}_{LS}(r)$ . The numerical results are shown with the tree level (dashed curve) and unitary (solid curve)  $\pi\pi$  correlation function. The gray area is the soft pion limit with quark masses  $M_q = 350$  (upper limit) to  $410$  MeV (lower limit). The dot-dashed curve corresponds the soft pion limit but with  $R_s$  related to the  $g_A$ . The dashed horizontal line represents the large- $N_c$  QCD expectation,  $1/\mathcal{R} = 9$ .

the short-distance expansion [48, 66]. This is the reason, why Eq. (54) so accurately represents the short-distance part of the CrTPE force. At the same time, it is very difficult to argue that the scaling of scalar-isoscalar nuclear forces, first predicted by Kaplan and Manohar [38], and the observation which we made here, are not accidental, because it is very difficult to justify any phenomenological models at such separation scales where the baryon number is not well defined [3, 67] and where other hard QCD processes [68] should play some role. We also recall that the  $\chi$ QSM itself as provided by the action Eq. (21) is valid for the values of the quark momenta up to the UV cut-off  $\Lambda = 1/\langle \rho \rangle \simeq 600$  MeV or  $r > r_\Lambda \simeq 0.3$  fm. In addition, we have to take into account the limited accuracy of the method used here to calculate  $\sigma(t)$ . Considering our findings as an empirical fact, we note that, other models, e.g. Ref. [26, 69], should be employed here to check our statements. To further support the scaling relation Eq. (54) we show in Fig. 7 the  $r$ -dependence of the inverse ratio  $1/\mathcal{R}(r) = \mathcal{V}_C(r)/\mathcal{V}_{LS}(r)$ . Indeed, the ratio  $\mathcal{V}_C(r)/\mathcal{V}_{LS}(r)$  scales according to

Eq. (54) forming a plateau up to distances  $r \simeq 0.8$  fm and fastly decreases beyond. The plateau covers the region where the action Eq. (21) is already reliable and the present approach is well justified.

A good agreement with the scaling relation is also found for the soft pion limit. For  $M_q = 350$  MeV and 410 MeV, Eqs. (44) and (51) result in  $\mathcal{R} \simeq 0.12$  and  $\simeq 0.16$ , respectively. The radial dependencies of the inverse ratios are shown in Fig. 7 by the band, where the upper limit corresponds to  $M_q = 350$  MeV and lower one to  $M_q = 410$  MeV. Additionally, due to the smallness of  $M_\pi^2 R_s^2$  in Eqs. (44) and (51), the following relation holds:  $\mathcal{R} \simeq (9/10)(M_q^2/M_N^2)$ . Using Eq. (24) with  $R_s = 1/M_q$  it can be written alternatively

$$1/\mathcal{R} \simeq \frac{5}{6} \left( \frac{g_A}{4\pi} \right) \frac{M_N^2}{f_\pi^2}. \quad (55)$$

With the empirical value for the axial coupling constant,  $g_A \simeq 1.25$ , Eq. (55) results in  $\mathcal{R} \simeq 0.12$  in good agreement with Eq. (54). The  $r$ -dependence of  $1/\mathcal{R}$  with the soliton size  $R_s$  related to the axial coupling constant  $g_A$ , Eq. (24), is shown in Fig. 7 by the dot-dashed curve.

## VII. SUMMARY

In summary, we have considered the effect of correlated two-pion exchange modes on the central and spin-orbit parts of the scalar-isoscalar  $NN$  interaction. We have coupled the  $\pi\pi$  correlation function to the scalar form factor of the nucleon which we calculated in the large- $N_c$  limit in the framework of  $\chi$ QSM. The CrTPE force obtained here confirms an unconventional behavior of scalar-isoscalar  $\pi\pi$  correlations in the  $NN$  interaction recently found in unitarized  $\chi$ PT [26]. For the central  $NN$  potential with, both, the tree level and unitary  $\pi\pi$  correlation functions we find a strong repulsive core at short ranges and a moderate attraction at intermediate distances. This result indicates that strong repulsive interactions can be generated by the pion-pion dynamics and scalar-quark densities themselves. The strength of the intermediate range attraction is insensitive to the variation of quark masses. The long-range tail of the central CrTPE  $NN$  potential is driven by the the  $\pi N$  sigma term and consistent with the effective  $\sigma$  meson exchange. In addition, we find a sizable and repulsive spin-orbit force which differs from the  $LS$  interaction generated by the effective  $\sigma$  meson in OBE models.

The large- $N_c$  behavior of the CrTPE potential was considered and consistency with large- $N_c$  QCD expectations was found. Both, the central and  $LS$  forces satisfy large- $N_c$  QCD counting

rules. We have shown that the spin-orbit part is  $\mathcal{O}(1/N_c^2)$  in strength relative to the central force resulting in the ratio  $\simeq 1/9$  suggested by the  $1/N_c$  expansion for  $N_c = 3$ . The latter is in agreement with our numerical analysis and with the Kaplan-Manohar large- $N_c$  power counting.

Analytical representations for the CrTPE forces in the soft pion limit in terms of elementary functions were derived and their chiral content was studied. It was shown that the latter consists of two terms. The first one is generated by the symmetry breaking part of the mesonic Lagrangian and vanishes in the chiral limit. The second one, which is non-vanishing in the chiral limit, does not contain any pion mass dependence and appears as a dominant force which drives all essential features of the CrTPE - the strong repulsion at short separations and the moderate attraction at intermediate distances. We also find that the soft pion limit provides an accurate representation of the CrTPE and compares well with direct numerical calculations.

In a forthcoming work the role played by the CrTPE in the  $NN$  interaction will be addressed again and it will be shown that the behavior found here and in Ref. [26] is an important ingredient to the  $NN$  interaction and appears to be clearly seen in peripheral  $NN$  phase shifts above the inelastic threshold.

We acknowledge the correspondence with J.R. Pelaez. This work was supported by the Landesforschungschwerpunkt Baden-Württemberg and the Bundesministerium für Bildung und Forschung (06TU201).

- 
- [1] Particle Data Group, Rhys. Rev. D **67**, 1 (2002)
  - [2] X. m. Jin and B. K. Jennings, Phys. Rev. C **54** (1996) 1427
  - [3] A. Faessler *et al.*, J. Phys. G **27** (2001) 1851; V. I. Kukulin *et al.*, Int. J. Mod. Phys. E **11** (2002) 1; I. T. Obukhovsky *et al.*, J. Phys. G **29**, 2207 (2003); V. I. Kukulin *et al.*, J. Phys. G **30**, 287 (2004), [arXiv:nucl-th/0308059](https://arxiv.org/abs/nucl-th/0308059)
  - [4] R. Machleidt, K. Holinde, Ch. Elster, Phys. Rep. **149**, 1 (1987)
  - [5] R. De Tourreil, B. Rouben and D. W. L. Sprung, Nucl. Phys. A **242**, 445 (1975)
  - [6] S. Weinberg, Phys. Lett. B **251**, 281 (1990); Nucl. Phys. B **363**, 3 (1991)
  - [7] C. Ordonez and U. van Kolck, Phys. Lett. B **291**, 459 (1992); C. Ordonez, L. Ray and U. van Kolck, Phys. Rev. Lett. **72**, 1982 (1994); Phys. Rev. C **53**, 2086 (1996)
  - [8] N. Kaiser, R. Brockmann and W. Weise, Nucl. Phys. A **625**, 758 (1997)

- [9] D. R. Entem and R. Machleidt, Phys. Rev. C **68**, 041001 (2003)
- [10] R. Higa and M. R. Robilotta, Phys. Rev. C **68**, 024004 (2003); R. Higa, M. R. Robilotta and C. A. da Rocha, [arXiv:nucl-th/0310011](https://arxiv.org/abs/nucl-th/0310011)
- [11] M. C. M. Rentmeester, R. G. E. Timmermans, J. L. Friar and J. J. de Swart, Phys. Rev. Lett. **82**, 4992 (1999)
- [12] E. Epelbaum, W. Glockle and U. G. Meissner, Eur. Phys. J. A **19**, 125 (2004)
- [13] A. D. Jackson, D. O. Riska and B. Verwest, Nucl. Phys. A **249**, 397 (1975)
- [14] H.-C. Kim, J. W. Durso and K. Holinde, Phys. Rev. C **49**, 2355 (1994)
- [15] N. Kaiser, S. Gerstendorfer and W. Weise, Nucl. Phys. A **637**, 395 (1998)
- [16] V. Bernard, N. Kaiser and U. G. Meissner, Int. J. Mod. Phys. E **4**, 193 (1995)
- [17] V. Bernard, N. Kaiser and U. G. Meissner, Nucl. Phys. A **615**, 483 (1997)
- [18] V. Bernard, N. Kaiser and U. G. Meissner, Phys. Lett. B **309**, 421 (1993)
- [19] J. A. Oller, E. Oset and J. R. Pelaez, Phys. Rev. Lett. **80**, 3452 (1998); Phys. Rev. D **59**, 074001 (1999) [Erratum-ibid. D **60**, 099906 (1999)]; A. Gomez Nicola and J. R. Pelaez, Phys. Rev. D **65**, 054009 (2002)
- [20] A. Dobado and J. R. Pelaez, Phys. Rev. D **56**, 3057 (1997)
- [21] J. y. He, Z. G. Xiao and H. Q. Zheng, Phys. Lett. B **536**, 59 (2002)
- [22] A. Dobado and J. R. Pelaez, Phys. Rev. D **47**, 4883 (1993); Q. Ang, Z. g. Xiao, H. Zheng and X. C. Song, Commun. Theor. Phys. **36**, 563 (2001)
- [23] G. Colangelo, J. Gasser and H. Leutwyler, Nucl. Phys. B **603**, 125 (2001); B. Ananthanarayan, G. Colangelo, J. Gasser and H. Leutwyler, Phys. Rept. **353**, 207 (2001)
- [24] J. Nieves and E. Ruiz Arriola, Phys. Lett. B **455**, 30 (1999); Nucl. Phys. A **679**, 57 (2000)
- [25] J. A. Oller and E. Oset, Nucl. Phys. A **620**, 438 (1997) [Erratum-ibid. A **652**, 407 (1999)]
- [26] E. Oset, H. Toki, M. Mizobe and T. T. Takahashi, Prog. Theor. Phys. **103**, 351 (2000); [arXiv:nucl-th/0011008](https://arxiv.org/abs/nucl-th/0011008)
- [27] M. Lacombe *et al.*, Phys. Rev. C **21** (1980) 861
- [28] R. B. Wiringa, V. G. J. Stoks and R. Schiavilla, Phys. Rev. C **51**, 38 (1995)
- [29] V. G. J. Stoks *et al.*, Phys. Rev. C **49**, 2950 (1994)
- [30] R. Machleidt, Phys. Rev. C **63**, 024001 (2001)
- [31] D. O. Riska, Nucl. Phys. A **710**, 55 (2002)
- [32] T. H. R. Skyrme, Nucl. Phys. **31**, 556 (1962)

- [33] E. M. Nyman and D. O. Riska, *Phys. Scripta* **34**, 533 (1986); *Phys. Lett. B* **203**, 13 (1988)
- [34] T. S. Walhout and J. Wambach, *Phys. Rev. Lett.* **67**, 314 (1991)
- [35] N. Kaiser and U. G. Meissner, *Phys. Lett. B* **233**, 457 (1989)
- [36] D. Diakonov, V. Y. Petrov and P. V. Pobylitsa, *Nucl. Phys. B* **306**, 809 (1988); D. Diakonov and V. Y. Petrov, *JETP Lett.* **43** (1986) 75 [*Pisma Zh. Eksp. Teor. Fiz.* **43** (1986) 57]
- [37] P. Schweitzer, *Phys. Rev. D* **69**, 034003 (2004), for other applications of  $\nabla U$  expansion method see  
P. Schweitzer, *Phys. Rev. D* **67**, 114010 (2003)
- [38] D. B. Kaplan and A. V. Manohar, *Phys. Rev. C* **56**, 76 (1997)
- [39] R. Kaiser and H. Leutwyler, *Eur. Phys. J. C* **17**, 623 (2000)
- [40] M. R. Robilotta and C. A. da Rocha, *Nucl. Phys. A* **615**, 391 (1997)
- [41] J. Gasser, M. E. Sainio and A. Svarc, *Nucl. Phys. B* **307**, 779 (1988)
- [42] C. M. Maekawa, J. C. Pupin and M. R. Robilotta, *Phys. Rev. C* **61**, 064002 (2000)
- [43] S. Scherer, [arXiv:hep-ph/0210398](https://arxiv.org/abs/hep-ph/0210398)
- [44] S. Kamefuchi, L. O’Raifeartaigh and A. Salam, *Nucl. Phys.* **28**, 529 (1961)
- [45] M. R. Robilotta, *Phys. Rev. C* **63**, 044004 (2001)
- [46] M. H. Partovi and E. L. Lomon, *Phys. Rev. D* **2**, 1999 (1970)
- [47] G. ’t Hooft, *Nucl. Phys. B* **72**, 461 (1974)
- [48] E. Witten, *Nucl. Phys. B* **160**, 57 (1979)
- [49] D. B. Kaplan and M. J. Savage, *Phys. Lett. B* **365**, 244 (1996)
- [50] T. D. Cohen and B. A. Gelman, *Phys. Lett. B* **540**, 227 (2002); M. K. Banerjee, T. D. Cohen and B. A. Gelman, *Phys. Rev. C* **65**, 034011 (2002); A. V. Belitsky and T. D. Cohen, *Phys. Rev. C* **65**, 064008 (2002); T. D. Cohen and D. C. Dakin, *Phys. Rev. C* **68**, 017001 (2003)
- [51] Y. Oh and W. Weise, *Eur. Phys. J. A* **4**, 363 (1999)
- [52] D. Diakonov and V. Y. Petrov, *Nucl. Phys. B* **272**, 457 (1986)
- [53] D. Diakonov and M. I. Eides, *JETP Lett.* **38**, 433 (1983) [*Pisma Zh. Eksp. Teor. Fiz.* **38**, 358 (1983)]
- [54] M. Wakamatsu, *Phys. Rev. D* **46**, 3762 (1992)
- [55] H. C. Kim, A. Blotz, C. Schneider and K. Goeke, *Nucl. Phys. A* **596**, 415 (1996)
- [56] D. Diakonov *et al.*, *Nucl. Phys. B* **480**, 341 (1996)
- [57] D. Diakonov, [arXiv:hep-ph/9602375](https://arxiv.org/abs/hep-ph/9602375)
- [58] M. M. Pavan *et al.*, *PiN Newslett.* **16**, 110 (2002), [arXiv:hep-ph/0111066](https://arxiv.org/abs/hep-ph/0111066)
- [59] M. G. Olsson, *Phys. Lett. B* **482**, 50 (2000)

- [60] The large- $N_c$  scaling of the  $\sigma$  mass,  $M_\sigma \sim \mathcal{O}(1)$  relies on a  $q\bar{q}$  nature of this state. See for other interpretations: J. R. Pelaez, Phys. Rev. Lett. **92**, 102001 (2004)
- [61] R. F. Dashen, E. Jenkins and A. V. Manohar, Phys. Rev. D **49**, 4713 (1994) [Erratum-ibid. D **51**, 2489 (1995)]
- [62] T. D. Cohen and W. Broniowski, Phys. Lett. B **292**, 5 (1992)
- [63] D.O.Riska and E.M.Nyman, Phys. Lett. B **183** (1987) 7; A. Abada, Z. Phys. A **358**, 85 (1997); D.O.Riska and K.Dannbom, Phys. Scripta **37**, 7 (1988)
- [64] A. Abada, J. Phys. G **22**, L57 (1996)
- [65] D. O. Riska and B. Schwesinger, Phys. Lett. B **229**, 339 (1989)
- [66] S. R. Beane, [arXiv:hep-ph/0204107](https://arxiv.org/abs/hep-ph/0204107)
- [67] M. M. Kaskulov, V. I. Kukulin and P. Grabmayr, Int. J. Mod. Phys. E **12**, 449 (2003); M. M. Kaskulov, V. I. Kukulin and P. Grabmayr, Few Body Syst. Suppl. **14**, 101 (2003); I. T. Obukhovsky, M. M. Kaskulov and P. Grabmayr, Few Body Syst. Suppl. **14**, 41 (2003)
- [68] M. M. Kaskulov and P. Grabmayr, Phys. Rev. C **67**, 042201(R) (2003); M. M. Kaskulov and P. Grabmayr, Phys. Rev. C **69**, 028201 (2004)
- [69] T. Inoue, V. E. Lyubovitskij, T. Gutsche and A. Faessler, Phys. Rev. C **69**, 035207 (2004)